IEEE Access
Multidisciplinary | Rapid Review | Open Access Journal

Received March 1, 2022, accepted March 18, 2022, date of publication March 24, 2022, date of current version April 1, 2022.

*Digital Object Identifier 10.1109/ACCESS.2022.3161932*

# Mitigation of the Electric and Magnetic Fields of 500-kV Overhead Transmission Lines

**ADEL Z. EL DEIN[1], OSAMA E. GOUDA[2], MATTI LEHTONEN[3], AND MOHAMED M. F. DARWISH[3,4], (Member, IEEE)**

[1]Department of Electrical Power Engineering, Faculty of Energy Engineering, Aswan University, Aswan 81528, Egypt
[2]Department of Electrical Power Engineering, Faculty of Engineering, Cairo University, Giza 12613, Egypt
[3]Department of Electrical Engineering and Automation, School of Electrical Engineering, Aalto University, 02150 Espoo, Finland
[4]Department of Electrical Engineering, Faculty of Engineering at Shoubra, Benha University, Cairo 11629, Egypt

Corresponding authors: Adel Z. El Dein (azeinm2001@hotmail.com) and Mohamed M. F. Darwish (mohamed.m.darwish@aalto.fi; mohamed.darwish@feng.bu.edu.eg)

This work was supported by the Department of Electrical Engineering and Automation, School of Electrical Engineering, Aalto University, Espoo, Finland.

**ABSTRACT** The electric and magnetic fields of overhead high voltage transmission lines are still a critical problem for new construction because of their biological effects on the human body. This issue has been a subject of scientific interest and public concern for the risk of the electric and magnetic fields on living organisms. Accordingly, the overhead transmission lines are considered a source of such this risk due to their high electric and magnetic fields in the populated areas. Because of the recent concerns that electric besides magnetic fields, generated by overhead transmission lines, electric power researchers have been trying to find effective methods for the mitigation of the electrical and magnetic fields to be in the range of acceptable limits. Researchers have been trying to find transmission line geometries that will reduce these electric and magnetic fields. Therefore, in this article two novel methods of reducing the electric and magnetic fields are discussed, one is to change the position of the center phase to optimize the delta configuration and the other is to use more than two shielding wires with calculating the currents in these wires. The obtained results of the two proposed methods are compared with the electric as well as magnetic fields, and the right-of-way values of the present conventional configuration. Additionally, this article presents a case study carried out on an Egyptian 500 kV high voltage overhead transmission line for the mitigation of magnetic and electric field intensities.

**INDEX TERMS** Mitigation of the electrical and magnetic fields, numerical methods, biological effects of electromagnetic, overhead power transmission lines.

## I. INTRODUCTION

The use of electrical energy transmission lines in populated areas causes numerous issues, that's due to the high value of the electric besides magnetic fields on the ground level which affects the men, animals, and plants, and also because most of the people have been concerned about possibly of their carcinogenic influences [1]. Possible danger to humans and animals' health from living near electrical energy transmission lines has been worried by scientists throughout the past years [1]. Electric field effects from overhead lines are caused by the extremely high voltage while magnetic field effects are due to line loading and short circuit currents. Exposure to 50-Hz electric and magnetic fields created by overhead lines has been expected of increasing the risk to living organisms [2]. One of the main key elements that determine the selection of transmission line right of way (ROW) is that the high impact of electric and magnetic fields. Power line ROW, in general, can be defined as the safe path of the overhead transmission lines (OHTLs) so that humans are not exposed to influential values of electric and magnetic fields while maintaining the continuous flow of electrical energy. Such as, for 230 kV, 500 kV, and double-circuit 500-kV lines, the supervisory staff selected magnetic field levels of 150, 200, and 250 mG edge of ROW magnetic field, respectively [3]. In another way, the ROW is described as the distance from the center phase into a point where the electric field at one meter directly above the ground level is considered to be 1.5 kV/m [4].

The supervisory staff's regulations establish the width of ROW necessary for a certain line design, or, opposite, what lines can be built on a particular ROW [2]. The magnetic

The associate editor coordinating the review of this manuscript and approving it for publication was Xiaodong Liang.

and electrical field values, as well as profiles around underneath overhead transmission lines, are known to be affected by the geometrical characteristics of these lines. Some of the researchers used a passive loop conductor to reduce the magnetic field. Moreover, the influence of active and passive shield wires on the magnetic field values below the lines as well as the electric field on the conductor's outer surface are underlined by reference [5]. Mitigation of magnetic field below overhead transmission line was done including the impacts of the sag between towers, as well as the sag variant with the temperature on the magnetic field calculations [6]. Safety assessment and lessening technology for extremely low frequency (ELF) of electromagnetic fields and guidelines for restricting exposure to time-varying electric and magnetic fields age were presented in references [7], [8]. A summary of the methods used in the mitigation of electric and/or magnetic fields was given in Table 1.

This article presents two methods for reducing the magnetic and electrical fields' values, one by changing the position of the center phase to optimize the delta configuration, which considers as an innovative method that has not been used before, and the other is by the use of more than one shielding wire. Investigation of the impact of the shielding wires' parameters namely, their numbers, their heights directly above the ground level, as well as the spacing between them on the electromagnetic fields of electrical energy transmission lines are done. The effects of the center phase position to optimize the delta configuration, both on the ROW and profiles of electric and magnetic fields at ground level have been investigated.

The Charge Simulation Method (CSM) is utilized for electric field computations [12], [13], the number and position of line charges are chosen to give the exact values of the electrical field under the transmission lines. The Biot-Savart law is used for magnetic field computations. The calculations of electromagnetic fields in case of changing the centerline position and in case of using shielding wires are compared with the using of the conventional 500 kV overhead transmission line configuration.

The study shows that the geometrical parameters of the three-phase configuration can be optimized to reduce the maximum ground electric and magnetic fields. Also, it is noticed that increasing the shielding wires by a number of more than two has little influence in reducing the electric and magnetic fields.

## II. ELECTRIC AND MAGNETIC FIELDS CALCULATION

Some assumptions are considered in the proposed methods of calculations, they are as the following:

1) The overhead transmission line is assumed to be infinitely long.

2) The overhead transmission line phase currents are assumed to be sinusoidal besides at balance condition. The mutual couplings between the transmission line phases are ignored.

**TABLE 1. Methods used in the mitigation of electric and magnetic fields of power lines.**

| Method | Method description | Drawbacks |
|---|---|---|
| Line compaction [9] | Reduction in phase spacing | May introduce corona; may limit available techniques for live line maintenance |
| Reverse phase (transposition) [10] | Reversal of phases on double circuit line | Only applicable to double circuit lines |
| Delta or reverse delta configuration [10] | Conversion from a flat configuration to delta | May introduce corona |
| Split phases [10] | Splitting of phases to create additional phases to create significant field reduction. | Increases complexity of line structures |
| Shielding with loops [11] | Conductive loop placed under the line | Increases complexity of the transmission system |

3) The electrical resistivity of the earth under the overhead transmission line is assumed to be constant.

### A. ELECTRIC FIELD CALCULATION

In this article, the charge simulation and image methods are employed to compute the electric field in the surrounding area of the 500 kV transmission line. In the traditional CSM, fictitious charges are applied to estimate the field in the nearby region under study. The position, as well as the type of these charges, are determined although their magnitudes are unidentified. Further, infinite line charges are utilized to model the systems that have translational equilibrium; therefore, they are applied to simulate the electric field of the multiphase ac overhead transmission lines including the shielding wires. Regarding, the three-phase transmission structures, the applied voltages on the three-phase OHTLs are considered sinusoidal and can be placed in phasor or static form as:

$$V_1 = V_{rms}\angle 0^o \tag{1}$$

$$V_2 = V_{rms}\angle 120^o \tag{2}$$

$$V_3 = V_{rms}\angle 240^o \tag{3}$$

The potential of the shielding wires is considered as zero voltage. Enforcing these potentials as boundary restrictions at a set of contour points sitting on the surfaces of the OHTLs including compensating conductors leads to a linear system of equations in the complex unknown charges. These equations have the following structure:

$$\sum_{j=1}^{n} P_{ij}Q_i = V_i \quad i = 1, 2, \ldots, n \tag{4}$$

in which $n$ represents the number of contour points and/or simulating charges, $P_{ij}$ represents the potential

coefficients [14], in addition, $Q_j$ represents the unknown simulating charges. Further, Equation (4) can be placed into a matrix structure as:

$$[P]\,[Q] = [V] \tag{5}$$

where;

- $[P]$ is defined as a square matrix containing the potential coefficients,
- $[Q]$ is defined as a complex vector of the unknown charges, and
- $[V]$ is defined as the vector of boundary conditions' voltages.

The line charges simulating the overhead transmission lines of the system under study are given by:

$$[Q] = [P]^{-1}\,[V] \tag{6}$$

For checking the simulation method accuracy, checkpoints, at locations other than those utilized for the contour points that are employed in the simulation procedure, are validated by using the static shape of the charges presented in equation (6). After fulfilling the solution-quality measures, the electric field strength, as well as potential at every point in the space, can be computed from analytical expressions as follows [14].

$$E_t = \sqrt{E_{vi}^2 + E_{hi}^2} \tag{7}$$

$$E_{hi} = \sum_{j=1}^{n} Q_j \cdot L_{ij} \tag{8}$$

$$E_{vi} = \sum_{j=1}^{n} Q_j \cdot K_{ij} \tag{9}$$

$$L_{ij} = (x_i - x_j)(1/A_{ij}^2 - 1/I_{ij}^2) \tag{10}$$

$$K_{ij} = (y_i - y_j)/A_{ij}^2 - (y_i + y_j)/I_{ij}^2 \tag{11}$$

$$V_i = \sum_{j=1}^{n} P_{ij} \cdot Q_j \tag{12}$$

$$I_{ij} = \sqrt{(x_i - x_j)^2 + (y_i - y_j)^2} \tag{13}$$

$$A_{ij} = \sqrt{(x_i - x_j)^2 + (y_i - y_j)^2} \tag{14}$$

in which;

- $E_{hi}$, $E_{vi}$ are the component of an electric field at the specified $i^{th}$ point in the horizontal plus vertical paths, respectively, (kV/m),
- $L_{ij}$, $K_{ij}$ are the horizontal plus vertical electric field coefficients at specified $i^{th}$ point, respectively,
- $V_i$ is the potential at the specified $i^{th}$ point, (V),
- $x_i$, $y_i$ are the coordinates of the $i^{th}$ boundary contour point, and
- $x_j$, $y_j$ are the coordinates of the $j^{th}$ line charge.

### B. MAGNETIC FIELD CALCULATION

The common practice, in the calculation of magnetic fields underneath OHTLs, is to assume that the overhead transmission lines are straight away horizontal wires of infinite length. By applying the Biot-Savart law, the magnetic field intensity $H$ at a specified point $P(x_i, y_i)$ has only an azimuthal component, which can be calculated by equation (15) [2]–[4];

$$H = \frac{I}{2\pi d}\vec{a}_\phi \tag{15}$$

where:

- $I$ is known as the flowing current in the conductor in root-mean-square (RMS) value of Ampere;
- $d$ is known as the distance from the conductor to a specified point P in meters;
- $\vec{a}_\phi$ is known as the unit vector in the azimuthal, $\phi$, direction.

Mostly, because the power transmission line has several conductors (more than 1), the overall summation of the magnetic fields by each line current must be computed at a specified point P repeatedly. Further, Fig. 1 depicts the magnetic field intensity components created by a three-conductor system carrying currents, and in the z-direction (perpendicular to the page and get out).

For AC overhead high voltage transmission lines, the line currents are sinusoidal varying with time at the specified power frequency. Accordingly, the induced magnetic field in the surrounding area of the power transmission lines as well differs at the power frequency and phase algebra can be utilized to combine numerous components, so that yield the amplitude of the mandatory magnetic field (horizontal in addition to vertical vectors).

For a three-phase system with one conductor per phase, current $I$ can be written as follows:

$$[I] = I_{rms}\angle 0^o, I_{rms}\angle 120^o, I_{rms}\angle 240^o] \tag{16}$$

One can take into consideration the magnetic field part affected by the image currents. Hence, the complex depth $\alpha$ of each conductor image current can be originated as presented in [15].

$$\alpha = \sqrt{2}\delta e^{-j\pi/4} \tag{17}$$

where;

$\delta$ is identified as the skin depth of the earth, which can be calculated by equation (18) [15].

$$\delta = 503\sqrt{\rho/f} \tag{18}$$

- $\rho$ is defined as the earth resistivity, and
- $f$ is defined as the source current frequency in Hz.

The magnetic field intensity at a specified point $P(x_i,y_i)$ induced from the passing current $I_i$ and its image is computed as follows:

$$\vec{H}_{ij} = H_{xij}\vec{a}_x + H_{yij}\vec{a}_y \tag{19}$$

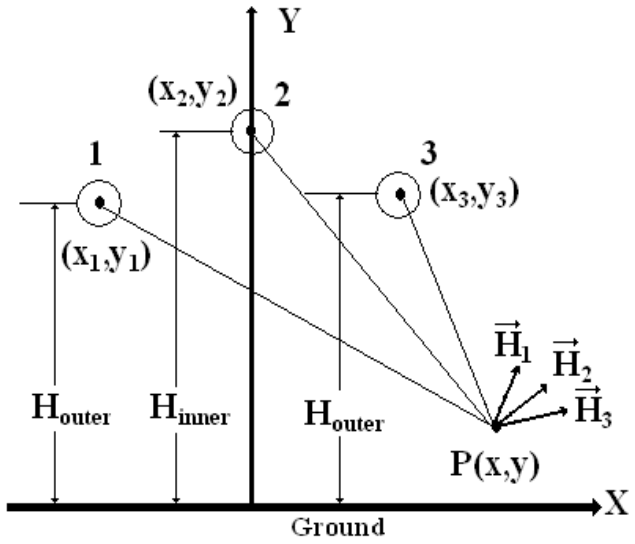


**FIGURE 1.** Magnetic field intensity components for 3 conductor system carrying currents.

$$H_{xij} = \frac{-I_j}{2\pi}\left[\frac{y_i - y_j}{r_{ij}^2} - \frac{y_i + y_j + \alpha}{r'^2_{ij}}\right] \tag{20}$$

$$H_{yij} = \frac{I_j}{2\pi}\left[\frac{x_i - x_j}{r_{ij}^2} - \frac{x - x_j}{r'^2_{ij}}\right] \tag{21}$$

where;

$\vec{a}_x$ represents the unit vector in the $x$-direction,
$\vec{a}_y$ represents the unit vector in the $y$-direction, and;

$$r_{ij} = \sqrt{(x_i - x_j)^2 + (y_i - y_j)^2} \tag{22}$$

$$r'_{in} = \sqrt{(x_i - x_j)^2 + (y_i + y_j + \alpha)^2} \tag{23}$$

The total summation of magnetic field intensity in the both $x$-and $y$-directions (i.e., horizontal and vertical components, respectively) are:

$$H_{xt} = \sum_{j=1}^{3} H_{xij} \tag{24}$$

$$H_{yt} = \sum_{j=1}^{3} H_{yij} \tag{25}$$

Finally, the magnitude of the resultant magnetic field intensity $H_t$ is:

$$H_t = \sqrt{H_{xt}^2 + H_{yt}^2} \tag{26}$$

Equations (20) and (21) are applicable in case of the distance away from the field point into the conductor is lesser than $\lambda/20$ where $\lambda$ is considered the free-space wavelength ($\lambda = c/f$ meters, where $c = 3 \times 10^8$ m/sec is the speed of the light). Furthermore, they are reasonable for any point above or near the ground outside the surface.

The current in the shielding wires can be calculated by using the multi-conductor transmission lines (MTL) technique, in which [16]:

$$\begin{bmatrix} \Delta V_p \\ \Delta V_G \end{bmatrix} = \begin{bmatrix} Z_{pp} & Z_{pG} \\ Z_{Gp} & Z_{GG} \end{bmatrix} \begin{bmatrix} I_p \\ I_G \end{bmatrix} \tag{27}$$

where; $\Delta V_p$ and $\Delta V_G$ are two vectors preset the drop along with the three phases and shielding wires respectively, $I_p$ and $I_G$ are three phases and shielding wires vectors currents respectively ($I_p = I$ in equation (16)), and $Z_{ij}$ is the per-unit series impedance (where $i$ and $j$ equal $p$ or $G$). $Z_{ij}$ can be calculated as follow:

$$Z' = j\omega L + Z_E + Z_{skin} \tag{28}$$

The external-inductance matrix is considering a frequency-independent real symmetric matrix with specified entries:

$$L_{ii} = \frac{\mu_o}{2\pi} \ln \frac{2y_i}{r_i} \tag{29.a}$$

$$L_{ij} = \frac{\mu_o}{4\pi} \ln \frac{(y_i + y_j)^2 + (x_i + x_j)^2}{(y_i - y_j)^2 + (x_i + x_j)^2} \tag{29.b}$$

Here $r_j$ symbolizes conductor radius, $y_j$ as well as $x_j$ represent the vertical and horizontal coordinates of the specified $j^{th}$ conductor, respectively.

The $Z_E$ represents the matrix of earth impedance correction and it is considered as a frequency-dependent complex matrix their entries can be obtained by using Carson's theory and/or by the approach of Dubanton complex ground plane [17]–[21]. Where the entries of $Z_E$ are calculated by:

$$(Z_E)_{jj} = j\omega \frac{\mu_o}{2\pi} \ln\left(1 + \frac{\alpha}{y_j}\right) \tag{30.a}$$

$$(Z_E)_{ij} = j\omega \frac{\mu_o}{4\pi} \ln\left(\frac{(y_i + y_j + 2\alpha)^2 + (x_i - x_j)^2}{(y_i - y_j)^2 + (x_i - x_j)^2}\right) \tag{30.b}$$

Here $\alpha$, is considered the complex depth, given in equation (17). The matrix of $Z_{skin}$ represents a frequency-dependent complex diagonal matrix with their entries that can be calculated by applying the skin-effect theory meant for cylindrical conductors [19]. For the instant of low-frequency situations, it becomes:

$$(Z_{skin})_{jj} = (R_{dc})_j + j\omega \frac{\mu_o}{8\pi} \tag{31}$$

in which $(R_{dc})_j$ indicates the dc resistance with per-unit-length of a specified $j^{th}$ conductor.

As the shielding wires are connected to earth (i.e., tower resistances are ignored), that outcome in: $\Delta V_G = 0$ then from equation (27), the induced shielding wires current can be calculated from the three-phase currents $I_p$ and $Z_{ij}$ matrix as follow;

$$I_G = \frac{-1}{Z_{GG}}(Z_{Gp} I_p) \tag{32}$$

The accuracy of a specific prediction of the electromagnetic fields under overhead transmission lines mainly depends on the reliability of the model into the actual situation [18], []19]. There are two categories of deviations from the actual situation. In the first case, the values of the model's parameters

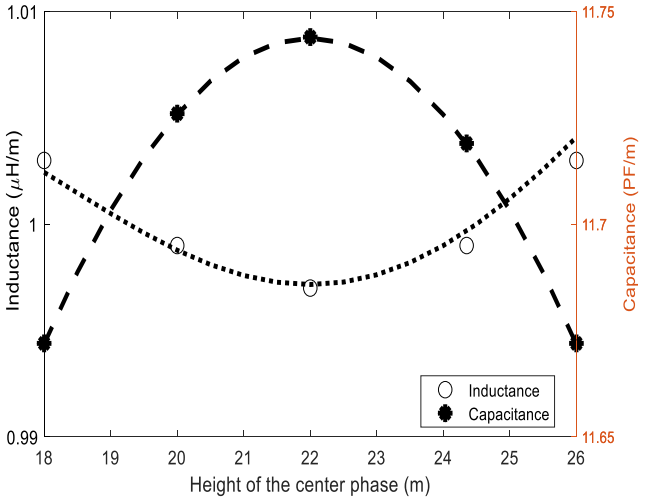


**FIGURE 2.** Variation in inductance and capacitance with the change in the middle phase position.

**TABLE 2.** Influences of the center phase heights on magnetic & electric fields and right-of-way.

| Center phase heights (m) | $E_{max}$ (kV/m) above one meter from the ground surface | ROW (m) | $E_{surf.\ Outer}$ (kV/m) On conductor surface | $E_{surf.\ Center}$ (kV/m) On conductor surface | $H_{max}$ (A/m) Above one meter from the ground surface |
|---|---|---|---|---|---|
| 18 | 6.216 | 37.29 | 419.254 | 460.526 | 30.852 |
| 20 | 4.831 | 36.97 | 422.619 | 457.55 | 27.439 |
| 22 | 4.855 | 36.69 | 424.804 | 454.325 | 25.392 |
| 24.35 | 4.9 | 36.44 | 425.742 | 448.863 | 24.004 |
| 26 | 4.938 | 36.3 | 425.455 | 443.679 | 23.432 |

may not be accurate. The amplitude of balanced currents, current asymmetry (phase and amplitude) incorporating shield wire currents, and earth resistivity are examples of these characteristics [21]–[28]. In this paper, the currents are assumed to be balanced in the three phases.

The second category consists of physical properties of the actual situation, which are not counted in the simplified model [29]–[32]. The most important of these are wires, pipes, towers, and non-homogeneous earth resistivity [33]–[38]. Some of these situations can be modeled in the above-mentioned magnetic field equations; others are more difficult to be represented.

As stated before, the aim of this article is to investigate two methods for mitigation of the electric and magnetic fields produced by 500-kV overhead lines, one is by the change of the position of the center phase of the delta configuration and the other is by using more than two shielding wires.

## III. RESULTS AND DISCUSSIONS

### A. CHANGING THE POSITION OF THE CENTER PHASE TO FORM DELTA CONFIGURATION

The effect of the change in the position of the middle phase conductor on the electrical characteristics of the line leads to changes in the phase inductance and capacitance. This is illustrated in Fig. 2. As it is noticed the phase inductance

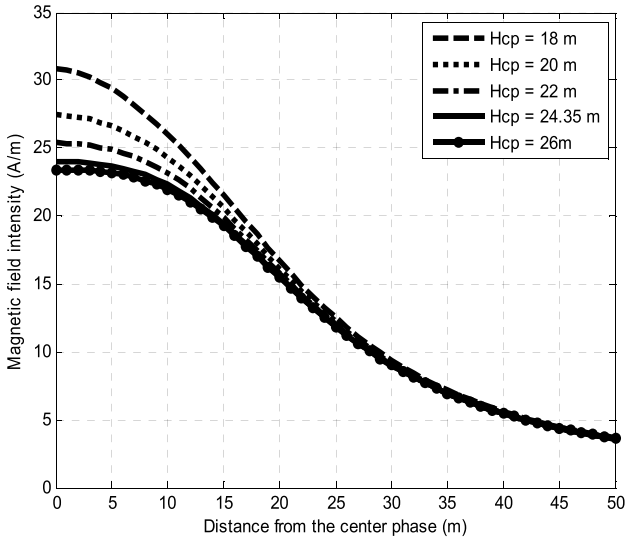


**FIGURE 3.** Effect of the centre phase height on the calculated magnetic field intensity of the 500 kV line.

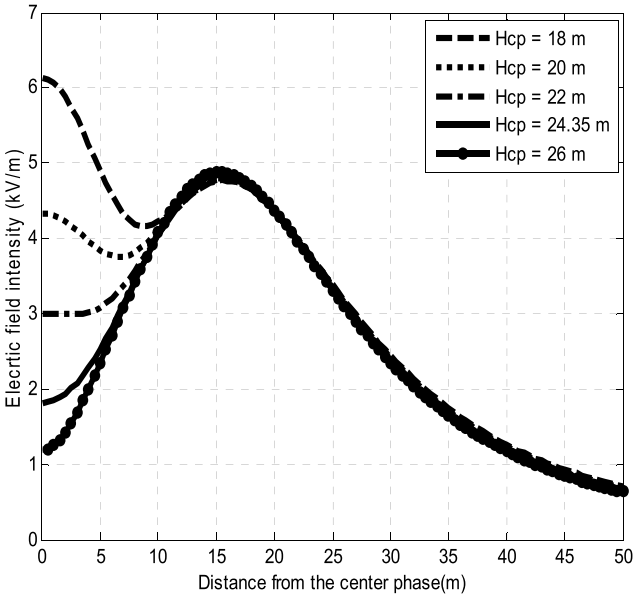


**FIGURE 4.** Effect of the centre phase height on the calculated electric field intensity.

is decreased, while at the same time the phase capacitance is increased. The variation in the line phase inductance and capacitance with the change in the middle phase position is considered in the electric and magnetic fields calculations.

To calculate the electric and magnetic field intensities at specified points one meter above the ground level for a 500 kV OHTLs, the data in appendix (A) are employed, besides the phase bundles are treated in terms of their corresponding radius [14]. The data given in Appendix A has been obtained regarding the El-Kuirmate-Cairo 500 kV power line, which is a part of the Egyptian overhead transmission line network [36]–[38].

Figures 3 and 4 show the variations of magnetic and electric fields intensities with the variation of the delta configuration center phase height. In this case, two ground wires

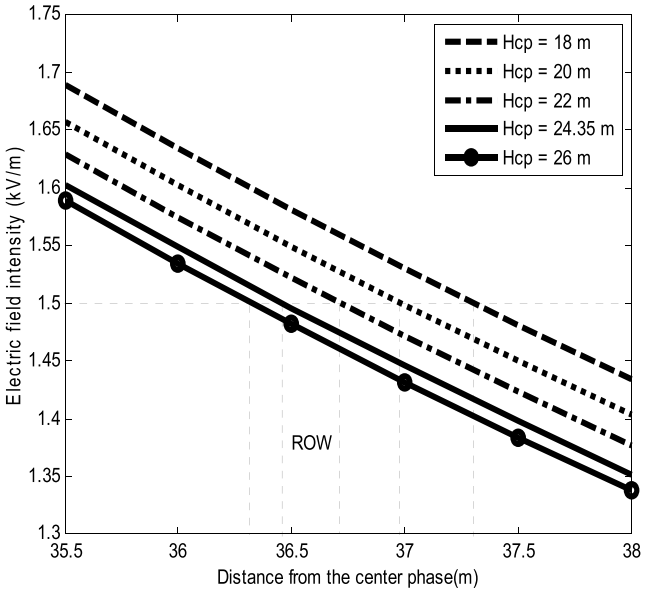


**FIGURE 5.** Variation of ROW with the centre phase height.

**TABLE 3.** Effect of the ground wires numbers on magnetic & electric fields and right-of-way.

| No. of Ground Wires | 0 | 1 | 2 | 3 | 4 |
|---|---|---|---|---|---|
| $E_{max}$ (kV/m) above one meter from the ground surface | 4.84 | 4.943 | 4.878 | 4.58 | 4.5274 |
| ROW (m) | 36.46 | 36.71 | 36.24 | 34.57 | 34.3 |
| $E_{Surf.Outer}$ (kV/m) On conductor surface | 425.93 | 422.588 | 425.088 | 435.3 | 437.6 |
| $E_{Surf.Center}$ (kV/m) On conductor surface | 449.37 | 463.313 | 458.871 | 470.71 | 462.16 |
| $H_{max}$ (A/m) above one meter from the ground surface | 24.0 | 23.3 | 23.07 | 22.31 | 23.68 |
| Induced ground currents (A) | - | 127.8 | 102.1<br>129.5 | 159.9<br>135.6<br>184.7 | 154.6<br>111.4<br>111.2<br>177.8 |

were positioned at the center of the tower, at height equals 30 m, and separation distance between them equals 7.5 m. Table 2 gives the influences of the center phase heights on both of magnetic and electric fields and ROW also. From Fig. 3 and Table 2 it is noted that, as it is expected, the maximum magnetic field decreases with the increase of the center phase height.

The maximum magnetic field is decreased from 30.852 (A/m) to 23.432 (A/m) with the increase of the center phase height from 18 m to 26 m. From Fig. 4, it is noticed that the maximum electric field intensity and its position are changed with the change of the center phase height. The maximum value of the electric field under the center phase reached (1.2 kV/m) when the center phase height was 26 m (higher than the outer phases by 4 m), while it was (6.13 kV/m) when the center phase height was 18 m (lower than the outer phases by 4 m). From 20 m to 26 m valuable

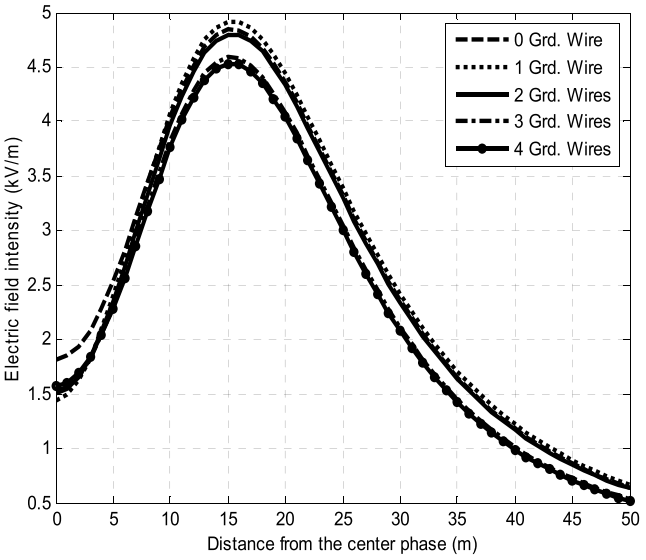


**FIGURE 6.** Effect of the shielding wires number on the calculated electric field intensity.

differences in electric field intensity values are noticed until the change of the center phase is done by about 8 meters (from 18 to 26 meters). Table 2, also shows the effect of the center phase height variation on the maximum electric and magnetic fields, ROW taking the safety limit of electric field (1.5 kV/m) [4] and outer and inner phases' surface gradient.

The maximum electric field decreases with the increase in the center phase height until distance (12 m) starting from the center phase as exposed in Fig. 3 in which the delta is changed to a flat configuration. Beyond this value, the maximum electric field intensity is slightly increasing at a distance of 15 m from the center phase with the increase of the center phase height.

As shown in Fig. 5 both of ROW and center phase surface gradient decrease with the increase in the center phase height, and finally the outer phases' surface gradient decreases with the increase in the center phase height as given in Table 2.

Finally, it is concluded that the maximum value of the electric field under the center phase is reduced to 19.57% of its value, the magnetic field intensity is reached to 76% of its value, and 3% reduction in the ROW of the overhead transmission lines is observed when the center phase height was 26 m rather than 18 m. As it is observed in Fig. 3, Fig. 4, and Table 2, the use of inverted delta configuration instead of flat formation or traditional delta can reduce the electric and magnetic fields on the ground level. The outer phases' surface gradient decreases with the increase in the center phase height as given in Table 2.

### *B. USING MORE THAN SHIELDING WIRE*

Figures 6 and 7 show the effect of the shielding wires' number on the calculated electric and magnetic fields, respectively. In this case, the original delta configuration was considered. The shielding wires were positioned at the center of the tower, at a height equal to 30 m, and there was a distance of 7.5 m between each adjacent two shielding wires.

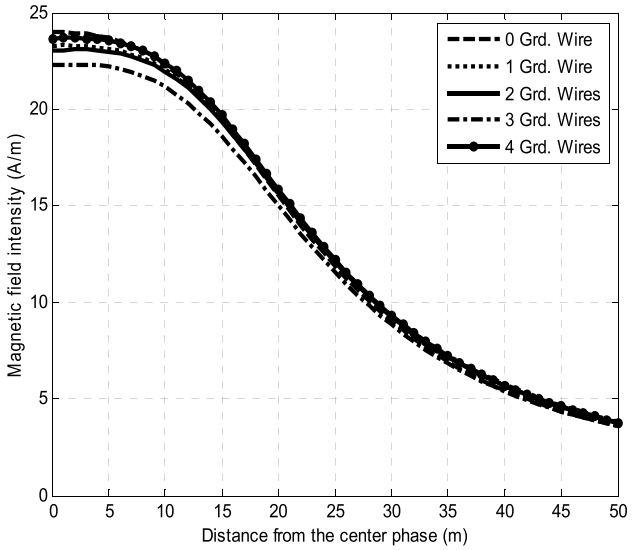


**FIGURE 7.** Effect of the shielding wires number on the calculated magnetic field intensity.

Table 3 illustrates the effect of the shielding wires' number on the maximum electric and magnetic fields, ROW, and outer and inner phases' surface gradient; also, this table presents the values of the induced currents in each shielding wire. Earth or shielding wires costs contain manufacturing and delivery of the shield wire to site and installation cost. According to Transmission Cost Estimation Guide MTEP19, the earth wire cost is 1,313 $ per each foot [39]. Increasing the earth wire number leads to an increase in the costs of installing the earth wires system.

From these results, it is noticed that and also from the economic point of view, the choice of two shielding wires is the best situation, where the maximum electric field, the ROW, and the center phase surface gradient have smaller values than those when the number of shielding wires equals one, three or even four, on the other hand, both the maximum magnetic field and the outer phase surface gradient decrease with the increase of the number of shielding wires, the choice of four shielding wires reduces the electric field by 8.1% than using two-wire shielding. On the other side, the magnetic field increases in the case of four shielding wires by 1.68% than using two shielding wires. The ROW decreases by about 2.6% when four shielding wires are used rather than the two wires. It is noticed also that the values of induced currents in (A) are unequal as given in Table 3. This is happened because of the phase differences between the currents carried by the phase conductors and the change in the space between shielding wires and phase conductors.

Tables 4 and 5 indicate the effect of the distance between the two shielding wires and their height, respectively on the maximum electric and magnetic fields, ROW, and outer and inner phases' surface gradient. It is observed that with the increase in the spacing between the two shielding wires; the maximum electric field decreases by about 3.3%, 5%, and 9% when the spacing between the two shielding conductors was 7 m, 9 m, and 15 m, respectively comparing with one meter spacing. Where the optimal separation distance between the two shield wires equals 13 m. Also, it is noticed that the ROW and the center phase surface gradient decrease, and the outer phase surface gradient increases.

**TABLE 4.** Effect of the distance between the two ground wires on magnetic & electric fields and right-of-way.

| Distance between the two ground wires (m) | $E_{max}$ (kV/m) above one meter from the ground surface | ROW (m) | $E_{Surf.Outer}$ (kV/m) On conductor surface | $E_{Surf.Center}$ (kV/m) On conductor surface | $H_{max}$ (A/m) above one meter from the ground surface |
|---|---|---|---|---|---|
| 1 | 4.939 | 37.12 | 418.960 | 482.029 | 23.216 |
| 3 | 4.918 | 37 | 419.704 | 480.237 | 23.114 |
| 5 | 4.857 | 36.66 | 422.503 | 471.930 | 23.082 |
| 7 | 4.776 | 36.18 | 426.543 | 463.069 | 23.081 |
| 9 | 4.686 | 35.58 | 431.213 | 455.884 | 23.094 |
| 11 | 4.601 | 34.9 | 435.690 | 450.897 | 23.117 |
| 13 | 4.532 | 34.24 | 438.919 | 447.991 | 23.079 |
| 15 | 4.489 | 33.68 | 440.168 | 446.715 | 23.189 |

**TABLE 5.** Effect of the two ground wires' height on magnetic and electric fields and right-of-way.

| Height of the two ground wires (m) | $E_{max}$ (kV/m) above one meter from the ground | ROW (m) | $E_{Surf.Outer}$ (kV/m) On conductor surface | $E_{Surf.Center}$ (kV/m) On conductor surface | $H_{max}$ (A/m) above one meter from the ground surface |
|---|---|---|---|---|---|
| 26 | 4.1284 | 32.5 | 466.5034 | 440.3731 | 23.004 |
| 27 | 4.2715 | 33.1 | 455.3972 | 443.0351 | 23.039 |
| 28 | 4.3803 | 33.5 | 447.9607 | 445.1156 | 23.076 |
| 29 | 4.4650 | 33.9 | 442.7275 | 446.7383 | 23.113 |
| 30 | 4.5319 | 34.24 | 438.9186 | 447.9908 | 23.079 |

The maximum magnetic field decreases by about 0.6%, 0.58%, and 0.11%, which are not valuable reductions, when the spacing between the shielding conductors was 7 m, 9 m, and 15 m, respectively compared with one meter spacing. Also, it is observed that; with the increase in the heights of the two shielding wires the maximum electric and magnetic fields, the ROW and the center phase surface gradient increase; and the outer phase surface gradient decreases.

## IV. CONCLUSION

The article gives modified algorithms to investigate the effect of the number of the shielding wires and the center phase position on the values of the electric and the magnetic fields, ROW, values of the induced current in the shielding wires conductors, and center and outer phase potential gradient. This article contains a case study carried out on an Egyptian 500 kV OHTL. Magnetic and electric fields' intensities at points one meter above the ground level are calculated. The obtained results of the two proposed methods are compared with the present electric and magnetic fields values of the conventional model. The calculations show that the number of the shielding wires and the center phase position which form inverted delta configuration instead of flat formation or

normal delta can reduce the electric and magnetic fields on the ground level, but the electric surface gradient on the phase conductors slightly increases.

It is concluded that the maximum values of the electric field and the magnetic field intensity under the center phase of the OHTL are reduced to 19.57% and 76% of their initial values respectively, 3% reduction in the ROW of the overhead transmission line is observed when the center phase height was 26 m rather than 18 m. It is noticed, also that with the increase in the spacing between the two shielding wires; the maximum electric field decreases by about 3.3%, 5%, and 9% when the spacing between the shielding conductors is 7 m, 9 m, and 15 m, respectively comparing with one meter spacing. The ROW and the center phase surface gradient decrease and the outer phase surface gradient increases. The maximum magnetic field decreases by about 0.6%, 0.58%, and 0.11%, which are not valuable reductions when the spacing between the shielding conductors was 7 m, 9 m, and 15 m, respectively.

## APPENDIX A

The calculations are done under three phases, single circuit, 500 kV TL, the following data of Egyptian 500 kV Kuirmate-Cairo power line are used [36]–[38] are used.

- The line-to-line voltage level: 500 kV (RMS)
- Rated power: 575 MVA
- Number of sub-conductors per phase: 3
- Diameter of a sub-conductor: 30.6 mm
- Spacing between sub-conductor in the bundle: 45 cm
- Minimum clearance to the ground: 9 m
- Height of the outer phases' conductors: 22 m
- Height of the center phase conductor: 24.35 m
- Diameter of compensating conductor: 11.2 mm
- Distance between adjacent two phases: 13.2 m
- Impedance per phase (positive and negative sequence): 3.307+ j 14.053 Ω
- Impedance per phase (Zero sequence): 10.75+j45.67 Ω
- Span: 400 m
- Line length: 124 km

## ACKNOWLEDGMENT

This work was supported by the Department of Electrical Engineering and Automation, School of Electrical Engineering, Aalto University, Espoo, Finland.

## REFERENCES

[1] T. S. Tenforde, *Biological Effects of Extremely-Low-Frequency Magnetic Fields, the Panel Session on Biological Effects of Power Frequency Electric and Magnetic Fields*, IEEE Standard 86THO139-6-PWR, 1986.

[2] *Guidelines for Limiting Exposure to Time-Varying Electric and Magnetic Fields (1Hz to 100 KHz)*, ICNIRP Guidelines, Germany, U.K., 2010.

[3] J. R. Stewart, S. J. Dale, and K. W. Klein, "Magnetic field reduction using high phase order lines," *IEEE Trans. Power Del.*, vol. 8, no. 2, pp. 628–636, Apr. 1993.

[4] A. Z. E. Dein, "Mitigation of magnetic field under Egyptian 500 KV overhead transmission line," in *Proc. 4th Int. Power Eng. Optim. Conf. (PEOCO)*, London, U.K., Jun. 2010, pp. 215–220.

[5] R. M. Radwan, A. M. Mahdy, M. Abdel-Salam, and M. M. Samy, "Electric field mitigation under extra high voltage power lines," *IEEE Trans. Dielectr. Electr. Insul.*, vol. 20, no. 1, pp. 54–62, Feb. 2013.

[6] Z. A. E. Dein, "Mitigation of magnetic field under overhead transmission line," in *Electrical Engineering and Applied Computing* (Lecture Notes in Electrical Engineering), vol. 90. Dordrecht, The Netherlands: Springer, Jun. 2011, pp. 67–81.

[7] *Research on Safety Assessment and Reduction Technology for ELF EMF*, Korea Electro-Technol. Res. Inst., Changwon, South Korea, 2008.

[8] R. W. P. King, "A review of analytically determined electric fields and currents induced in the human body when exposed to 50–60-Hz electromagnetic fields," *IEEE Trans. Antennas Propag.*, vol. 52, no. 5, pp. 1186–1192, May 2004.

[9] A. A. Dahab, F. K. Amoura, and W. S. Abu-Elhaija, "Comparison of magnetic-field distribution of noncompact and compact parallel transmission-line configurations," *IEEE Trans. Power Del.*, vol. 20, no. 3, pp. 2114–2118, Jul. 2005.

[10] P. Pretorius, "Electric and magnetic fields form overhead power Lines—A summary of technical and biological aspects," Eskom Holdings LTD, Sandton, South Africa, Final Rep., Aug. 2006, pp. 1–43. Accessed: Dec. 1, 2021. [Online]. Available: https://www.eskom.co.za/OurCompany/SustainableDevelopment/EnvironmentalImpactAssessments/Documents/Anderson_Substation_Appendix_C_-_Electric_and_Magnetic_Fields_from_Overhead_Power_Lines1.pdf

[11] K. Yamazaki, T. Kawamoto, and H. Fujinami, "Requirements for power line magnetic field mitigation using a passive loop conductor," *IEEE Trans. Power Del.*, vol. 15, no. 2, pp. 646–651, Apr. 2000.

[12] N. H. Malik, "A review of the charge simulation method and its applications," *IEEE Trans. Electr. Insul.*, vol. 24, no. 1, pp. 3–20, Feb. 1989.

[13] M. A. Habib, M. A. G. Khan, M. K. Hossain, and S. A. Hossain, "Investigation of electric field intensity and degree of uniformity between electrodes under high voltage by charge simulation method," in *Proc. 17th Int. Conf. Comput. Inf. Technol. (ICCIT)*, Dec. 2014, pp. 185–191.

[14] B. Anggoro and A. Qodir, "The induced current density calculation by charge simulation method for grounded and isolated man model exposed under 500 kV transmission line," in *Proc. Int. Conf. Electr. Eng. Comput. Sci. (ICEECS)*, Nov. 2014, pp. 269–273.

[15] H. Singer, H. Steinbigler, and P. A. Weiss, "A charge simulation method for the calculation of high voltage fields," *IEEE Trans. Power App. Syst.*, vol. PAS-93, no. 5, pp. 1660–1668, Sep. 1974.

[16] G. J. Anders, G. L. Ford, and D. J. Horrocks, "The effect of magnetic field on optimal design of a rigid-bus substation," *IEEE Trans. Power Del.*, vol. 9, no. 3, pp. 1384–1390, Jul. 1994.

[17] J. A. B. Faria and M. E. Almeida, "Accurate calculation of magnetic-field intensity due to overhead power lines with or without mitigation loops with or without capacitor compensation," *IEEE Trans. Power Del.*, vol. 22, no. 2, pp. 951–959, Apr. 2007.

[18] T. Noda, "A double logarithmic approximation of Carson's ground-return impedance," *IEEE Trans. Power Del.*, vol. 21, no. 1, pp. 472–479, Jan. 2006.

[19] A. Ramirez and F. Uribe, "A broad range algorithm for the evaluation of Carson's integral," *IEEE Trans. Power Del.*, vol. 22, no. 2, pp. 1188–1193, Apr. 2007.

[20] R. D. Begamudre, *Extra High Voltage A.C. Transmission Engineering*, vol. 7, 3rd ed. Hoboken, NJ, USA: Wiley, 2006, pp. 172–205.

[21] Y.-L. Ke and J.-C. Chiang, "Analysis and mitigation of the electromagnetic coupling problem associated with multi-conductors in three-phase systems," in *Proc. IEEE Ind. Commercial Power Syst. Tech. Conf.*, Apr./May 2006, pp. 1–10.

[22] R. Amiri, H. Hadi, and M. Marich, "The influence of sag in the electric field calculation around high voltage overhead transmission lines," in *Proc. IEEE Conf. Electr. Insul. Dielectr. Phenomena*, Oct. 2006, pp. 206–209.

[23] A. Z. El-Dein, A. A. W. Wahab, M. M. Hamada, and T. H. Emmary, "The effects of the span configurations and conductor sag on the electric-field distribution under overhead transmission lines," *IEEE Trans. Power Del.*, vol. 25, no. 4, pp. 2891–2902, Oct. 2010.

[24] A. V. Mamishev, R. D. Nevels, and B. D. Russell, "Effects of conductor sag on spatial distribution of power line magnetic field," *IEEE Trans. Power Del.* vol. 11, no. 3, pp. 1571–1576, Jul. 1996.

[25] A. Z. El-Dein, "Magnetic-field calculation under EHV transmission lines for more realistic cases," *IEEE Trans. Power Del.*, vol. 24, no. 4, pp. 2214–2222, Sep. 2009.

[26] Y. Yang, J. Lu, and Y. A. Lei, "A calculation method for the electric field under double-circuit HVDC transmission lines," *IEEE Trans. Power Del.*, vol. 23, no. 4, pp. 1736–1742, Oct. 2008.

[27] S. Carsimamovic, Z. Bajramovic, M. Rascic, M. Veledar, E. Aganovic, and A. Carsimamovic, "Experimental results of ELF electric and magnetic fields of electric power systems in Bosnia and Herzegovina," in *Proc. IEEE EUROCON-Int. Conf. Comput. Tool*, Apr. 2011, pp. 1–4.
[28] M. Z. A. Ab-Kadir and I. Cotton, "Application of the insulator coordination gap models and effect of line design to backflashover studies," *Int. J. Elect. Power Energy Syst.*, vol. 32, no. 5, pp. 443–449, Jun. 2010.
[29] D. D. Micu, L. Czumbil, G. C. Christoforidis, and A. Ceclan, "Layer recurrent neural network solution for an electromagnetic interference problem," *IEEE Trans. Magn.*, vol. 47, no. 5, pp. 1410–1413, May 2011.
[30] A. Ametani, "Four-terminal parameter formulation of solving induced voltages and currents on a pipeline system," *IET Sci., Meas. Technol.*, vol. 2, no. 2, pp. 76–87, Mar. 2008.
[31] D. A. Tsiamitros, G. C. Christoforidis, G. K. Papagiannis, D. P. Labridis, and P. S. Dokopoulos, "Earth conduction effects in systems of overhead and underground conductors in multilayered soils," *IEE Proc.-Gener., Transmiss. Distrib.*, vol. 153, no. 3, pp. 291–299, May 2006.
[32] R. Vajeth and D. Dama, "Conductor optimisation for overhead transmission lines," in *Proc. 7th Africon Conf. Afr.*, vol. 1, Sep. 2004, pp. 589–595.
[33] R. D. Southey, F. P. Dawalibi, and W. Vukonich, "Recent advances in the mitigation of AC voltages occurring in pipelines located close to electric transmission lines," *IEEE Trans. Power Del.*, vol. 9, no. 2, pp. 1090–1097, Apr. 1994.
[34] J.-B. Kim, "Comparison of electrical environmental characteristics of different EHV transmission lines," in *Proc. 11th Int. Symp. High-Voltage Eng. (ISH)*, Jul. 1999, pp. 262–265.
[35] M. A. Abouelatta, S. A. Ward, A. M. Sayed, K. Mahmoud, M. Lehtonen, and M. M. F. Darwish, "Fast corona discharge assessment using FDM integrated with full multigrid method in HVDC transmission lines considering wind impact," *IEEE Access*, vol. 8, pp. 225872–225883, 2020.
[36] *Egyptian Holding Company of Electricity Transmission*, Egyptian Electr. Holding Company, 2017, pp. 42–49. Accessed: Jul. 12, 2021. [Online]. Available: http://www.moee.gov.eg/english_new/EEHC_Rep/2016-2017en.pdf
[37] O. E. Gouda, A. Z. E. Dein, and M. A. H. El-Gabalawy, "Effect of electromagnetic field of overhead transmission lines on the metallic gas pipe-lines," *Electr. Power Syst. Res.*, vol. 103, pp. 129–136, Oct. 2013.
[38] N. M. K. Abdel-Gawad, A. Z. E. Dein, and M. Magdy, "Mitigation of induced voltages and AC corrosion effects on buried gas pipeline near to OHTL under normal and fault conditions," *Electr. Power Syst. Res.*, vol. 127, pp. 297–306, Oct. 2015.
[39] *Transmission Cost Estimation Guide MTEP19, 20190212 PSC Item 05a Transmission Cost Estimation Guide for MTEP 2019_for review317692.pd*. Accessed: Mar. 1, 2022. [Online]. Available: https://cdn.misoenergy.org/20190212%20PSC%20Item%2005a%20Transmission%20Cost%20Estimation%20Guide%20for%20MTEP%202019_for%20review317692.pdf

**ADEL Z. EL DEIN** was born in Egypt, in 1971. He received the B.Sc. and M.Sc. degrees in electric engineering from the Faculty of Energy Engineering, Aswan, Egypt, in 1995 and 2000, respectively, and the Ph.D. degree in electric engineering from Kazan State Technical University, Kazan, Russia, in 2005. From 1997 to 2002, he worked as a Teaching Assistant with the Faculty of Energy Engineering. From 2002 to 2005, he was with the Kazan Energy Institute, Kazan, and Kazan State Technical University. From 2005 to 2011, he was a Staff Member with the Department of High Voltage Networks, Faculty of Energy Engineering, Aswan University, Aswan, where he was an Associate Professor, from 2011 to 2016. In 2014, he joined the Department of High Voltage Engineering (Hikita Laboratory), Kyushu Institute of Technology (KIT), Japan, as a Researcher. Since 2016, he has been a Full Professor in high voltage engineering with the Department of High Voltage Networks, and the Dean of the Faculty of Energy Engineering, Aswan University. His research interests include calculation of electric and magnetic fields and their effects, and comparison of numerical techniques in electromagnetics. He is a Regular Reviewer of IEEE TRANSACTIONS ON POWER DELIVERY, ELECTRIC POWER SYSTEMS RESEARCH, and *IET Generation, Transmission & Distribution*.

**OSAMA E. GOUDA** was born in 1951. He received the B.Sc. degree in electrical engineering and the M.Sc. and Ph.D. degrees in the field of high voltage from Cairo University, Egypt, in 1975, 1979, and 1982, respectively. From 1988 to 1993, he was an Associate Professor with the Department of Electrical Power Engineering, Faculty of Engineering, Cairo University. In 1988, he was with the Department of Electrical Engineering, Kema Institute, Arnhem, The Netherland, where he was a Research Fellow. Since 1993, he has been a Full Professor with the Electrical Engineering Department, Cairo University, where he is currently the Head of the High Voltage Group, Electrical Power Engineering Department. He has published more than 140 papers and he was a supervisor for about 70 M.Sc. and Ph.D. degrees. His research interests include the high-voltage phenomena, cable insulation, protection of power systems, and electromagnetic transients.

**MATTI LEHTONEN** received the master's and Licentiate degrees in electrical engineering from the Helsinki University of Technology, Finland, in 1984 and 1989, respectively, and the Ph.D. degree in technology from the Tampere University of Technology, Finland, in 1992. He was with VTT Energy, Espoo, Finland, from 1987 to 2003. Since 1999, has been a Full Professor and the Head of the Power Systems and High Voltage Engineering Group, Aalto University, Espoo. His research interests include power system planning and assets management, power system protection, including earth fault problems, harmonic related issues, high voltage systems, power cable insulation, and polymer nanocomposites. He is an Associate Editor of *Electric Power Systems Research* and *IET Generation, Transmission & Distribution*.

**MOHAMED M. F. DARWISH** (Member, IEEE) was born in Cairo, Egypt, in 1989. He received the B.Sc., M.Sc., and Ph.D. degrees in electrical engineering from the Faculty of Engineering at Shoubra, Benha University, Cairo, Egypt, in May 2011, June 2014, and January 2018, respectively. From 2016 to 2017, he joined Aalto University, Finland, as a Ph.D. student with the Department of Electrical Engineering and Automation (EEA) and the Prof. M. Lehtonen's Group. He is currently working as an Assistant Professor with the Department of Electrical Engineering, Faculty of Engineering at Shoubra, Benha University. He is also a Postdoctoral Researcher with the Department of EEA, School of Electrical Engineering, Aalto University. He has coauthored in several international IEEE journals and conferences. His research interests include HV polymer nanocomposites, nano-fluids, electromagnetic fields, partial discharge, dissolved gas analysis, fault diagnosis, renewables, optimization, the IoT, and industry 4.0. He received the Best Ph.D. Thesis Prize that serves Industrial Life and Society all over the Benha University Staff for the academic year (2018–2019). Since 2021, he has been a Topic Editor of *Catalysts* (MDPI) journal, and also becomes a Guest Editor for the special issue in *Catalysts* (MDPI) journal. Further, in 2022, he has nominated as a Topic Editor of *Frontiers in Energy Research* journal.